iJRASET
International Journal For Research in Applied Science and Engineering Technology

INTERNATIONAL JOURNAL FOR RESEARCH

IN APPLIED SCIENCE & ENGINEERING TECHNOLOGY

Volume: 8 **Issue:** VII **Month of publication:** July 2020

DOI: https://doi.org/10.22214/ijraset.2020.30446

www.ijraset.com

Call: 08813907089 | E-mail ID: ijraset@gmail.com

International Journal for Research in Applied Science & Engineering Technology (IJRASET)
ISSN: 2321-9653; IC Value: 45.98; SJ Impact Factor: 7.429
Volume 8 Issue VII July 2020- Available at www.ijraset.com

Implementation of DVR for the better Voltage Profile in PV System

N. Manasa[1], M. Sekhar[2]
[1]*P.G. Student, Department of EEE, P.V.K.K. Institute of Technology,*
[2]*Assistant Professor, Department of EEE, P.V.K.K. Institute of Technology,*

Abstract: ***Switching losses in a grid connected Photovoltaic system are mitigated through the adaption of a Dynamic Voltage Restorer (DVR) as described in this paper. Generally the issue of symmetrical and asymmetrical grid faults coupled with voltage swell and sags are the common areas of concern in the operation of the grid. Renewable energy source, as a standby is considered, to cater to the losses. As the system of PV generation has the multi stage rectifiers and the maximum power point tracking, these help in registering the improvement in overall functionality of the grid. With the charging of dc link capacitor through load side shunt rectifier, the problems of maintaining rated voltage at DVR, inability to supply active power through PV plant, is addressed there by ensuring continuity in supply. A six port converter for integrating onsite PV generation and the DVR eliminates individual inverters for each of PV system and DVR resulting in reduced switching losses, with better utilization. The proposed configured system will prove to be useful for power load canters up to medium capacity with considerable onsite generation through PV system. Keywords: Bidirectional Power Flow, Distributed Power Generation, Photovoltaic System, Power Quality, Voltage Control.***

Keywords: Dynamic Voltage Restorer (DVR), Power quality, Voltage profile, PV System, Voltage control.

I. INTRODUCTION

Environmental pollution concerns have shifted the focus of the world towards alternate energy sources, especially of renewable nature like Photo Voltaic and wind Energy. The dc generation of a PV source requires an inversion to ac for suitability to be coupled to a grid. The volt-ampere rating of the inverter is based on the rating of the solar panels and to determine as such is tricky, as the generation is intermittent and the utilization factor of the associated equipment like DVR would be less, typically between 20% to 40 %. In the proposed configuration, the inverters at PV side and DVR side are amalgamated to reduce the switch count by about 25% thereby overcoming the operational difficulties as mentioned above and thus could be useful for low to medium load centres with greater proportion of generation through onsite PV source.

Table I Different modes of operation – proposed PV-DVR scheme. Fig 1 Fig 1 Since the volt-ampere rating of the PV system governs the rating of associated six port converter and DVR, any deficit by the source voltage in catering to the load, can be fulfilled by the renewable energy source, in our case a PV source. Appropriate sized filters are employed to mitigate the harmonics at the point of coupling for smoother conversion of DC-AC. For deeper sag, with current requirements exceeding the ratings of the switches, the capacitor is sized based on the following Equ. (1).

TABLE I.
Integrated PV-DVR System Configuration: Different Modes Of Operation

Mode	PV status	Grid condition	Switch status		Six-port converter operation	
			Always "ON"	PWM	PV-VSI	DVR-VSI
1	Active	Healthy $V_{pcc-p.u.} = 1$	S_7–S_9	S_1–S_6	Active ($P_{PV\text{-}VSI} > 0$)	Idle ($PQ_{DVR\text{-}VSI} = 0$)
2	Active	Fault $V_{pcc-p.u.} \approx 0$	S_1–S_3	S_4–S_9	Idle ($P_{PV\text{-}VSI} = 0$)	Active ($PQ_{DVR\text{-}VSI} = PQ_{LOAD}$)
3	Active	Sag $0.1 < V_{pcc-p.u.} < 0.95$	None	S_1–S_9	Active ($P_{PV\text{-}VSI} > 0$)	Active ($PQ_{DVR\text{-}VSI} < PQ_{LOAD}$)
4	Inactive	Any of the above 3	None	S_1–S_9	Active ($P_{PV\text{-}VSI} < 0$)	Active

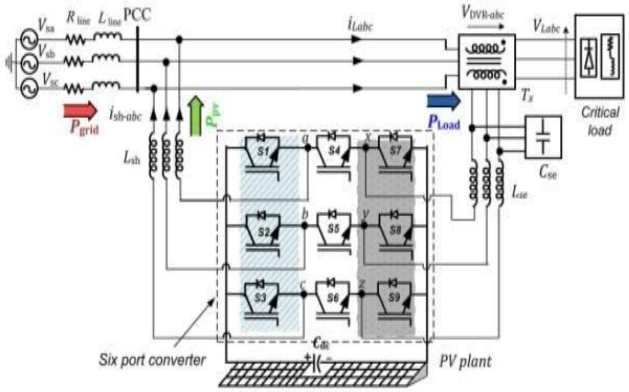

Fig1. Power Generation from PV and Transmission to Load.

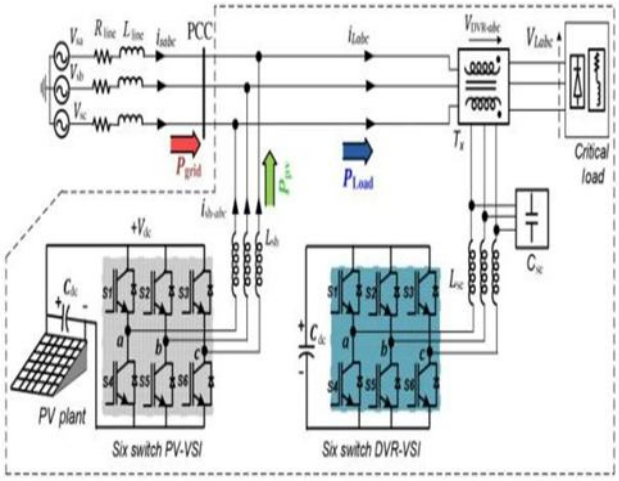

Fig2. Proposed combined PV and DVR system configuration.

$$C_d = \frac{t_{c-\max} * 2 * P_{dvr-vsi}}{\left[V_{dc}^2 - \left(\frac{2 * V_{dvr-vsi}}{m_{i-\max} * n_t} \right) \right]} \qquad (1)$$

II. OPERATING PRINCIPLE FOR SIX PULSE CONVERTER

Three switches share the PV and DVR – VSI, of the six port converter as given in Fig 2. The four feasible connections on the same leg , of the two output ports are : 1) outputs connected to +V dc (for phase- a: S 1 -ON, S 4 -ON, and S 7 -OFF); 2) outputs to 0 V (for phase-a: S 1 -OFF, S 4 -ON, and S 7 -ON); 3) left port to +V dc and right port to 0 V (for phase-a: S 1 -ON, S 4 -OFF, and S 7 -ON) and 4) left port to 0 V and right port to +V dc (for phase-a: S 1 -ON, S 4 -ON, and S 7 -ON). However the 4th connection is omitted as this will result in direct short circuit of the dc link. Comparing the reference signals with common carrier, the gate pulses are generated for achieving modulation and their positioning left over right is based on the third harmonic injection method. The limitation of case 4 above causing a short circuit is avoided by indulging in the either of the two types of operation, i.e. 1) Equal frequency operation (as in Fig 3 a) or 2) Variable frequency operation (as in Fig 3 b) FIG 3 PV-VSI injects active power into the grid during Normal Mode (1) while DVR-VSI is idle with unity modulation index for PV-VSI other being zero , as in Fig 3(c). In Mode (3) the PV-VSI injects active power as in Mode (1), but at a reduced modulation index, because of reduction in PCC voltage due to sag, resulting in DVR-VSI to attain higher modulation index as in Fig. 3(d). The DVR-VSI reference and in PV-VSI reference are inversely related and hence the crossover does not happen.

Thus, the proposed configuration naturally overcomes the limitation of reference crossover. This process and procedure is to generate nine gate pluses is discussed below : Formula With the designations as a) $V_{pv\text{-}abc}$ and $V_{dvr\text{-}xyz}$ are the PV-VSI and DVR-VSI reference signals as determined by the respective control blocks (as detailed in Section IV), b) mpv , wpv , and ϕpv are the modulation ratio, angular frequency, and phase angle of the PV-VSI , c) mdvr , wdvr , and ϕdvr are the corresponding values for DVR-VSI, respectively.

$$V^{*}_{pv-a} = m_{pv}\,\mathrm{Cos}\left(\omega_{pv}t + \phi_{pv}\right)$$
$$V^{*}_{pv-b} = m_{pv}\,\mathrm{Cos}\left(\omega_{pv}t - 120^{0} + \phi_{pv}\right)$$
$$V^{*}_{pv-c} = m_{pv}\,\mathrm{Cos}\left(\omega_{pv}t - 240^{0} + \phi_{pv}\right) \quad (2)$$
$$V^{*}_{dvr-x} = m_{dvr}\,\mathrm{Cos}\left(\omega_{dvr}t + \phi_{dvr}\right)$$
$$V^{*}_{dvr-y} = m_{dvr}\,\mathrm{Cos}\left(\omega_{dvr}t - 120^{0} + \phi_{dvr}\right)$$
$$V^{*}_{dvr-z} = m_{dvr}\,\mathrm{Cos}\left(\omega_{dvr}t - 240^{0} + \phi_{dvr}\right) \quad (3)$$

The offsets references as modified are determined from (2) and (3) (2) (3) The 120 deg. discontinuous offset reference signals are given by $M_{pv\text{-}abc}$ and $M_{dvr\text{-}xyz}$ when fed to PWM comparators give two sets of six gating signals respectively .Where in Mc is the amplitude of the carrier signal. The six port converter has the middle row switches, which are shared, has the gating pulses generated by logical OR of the PWM signals corresponding to Gpv4 – 6 and Gdvr1-3. The nine gating signals are therefore obtained in Eqn. (8).

$$V_{n} = 1 - \left[Max\left(V^{*}_{pv-abc}\right)\right]$$
$$M_{pv-abc} = V_{n} + V^{*}_{pv-abc} \quad (4)$$
$$V_{m} = -1 - \left[Min\left(V^{*}_{dvr-xyz}\right)\right]$$
$$M_{dvr-xyz} = V_{n} + V^{*}_{dvr-xyz} \quad (5)$$
$$G_{pv1-3} = G_{pv4-6}\{1, if\ M_{pv-abc} > M_{c}$$
$$0,\ if\ M_{pv-abc} < M_{c} \quad (6)$$
$$G_{dvr1-3} = G_{dvr4-6}\{1, if\ M_{dvr-xyz} > M_{c}$$
$$0,\ if\ M_{dvr-xyz} < M_{c} \quad (7)$$
$$G_{n1-3} = G_{pv1-3}$$
$$G_{n7-9} = G_{dvr4-6}$$
$$G_{n4,5,6} = G_{pv4-6} + G_{dvr1-3} \quad (8)$$

III.OVERALL CONTROL SYSTEM

Control of PV-VSI The reactive and active power of PV-VSI in the synchronous frame of reference is expressed as (9) Using the voltage oriented control [5], the reference frame d-axis and positive sequence PCC voltage, are aligned i.e., $V_{d} = V_{pcc}$ Therefore, i_{dpv} giving a direct measure of PV power, and expressed as: (10) With i_{dpv}, as obtained from MPPT , the limitation of reference cross over is over come and the procedure for generation of nine gate pulses is now discussed: The sum of modulation reference not exceeding unity[8] , the reference signals are expressed as in fig 7(b) with the VF operation requiring doubling of dc link voltage preventing reference cross over.

$$P = 1.5 * \left[V_{d} i_{d} + V_{q} i_{q}\right]$$
$$Q = 1.5 * \left[V_{d} i_{d} - V_{q} i_{q}\right] \quad (9)$$
$$i^{*}_{d-pv} = \frac{2}{3 * V_{d}} P_{pv} \quad (10)$$

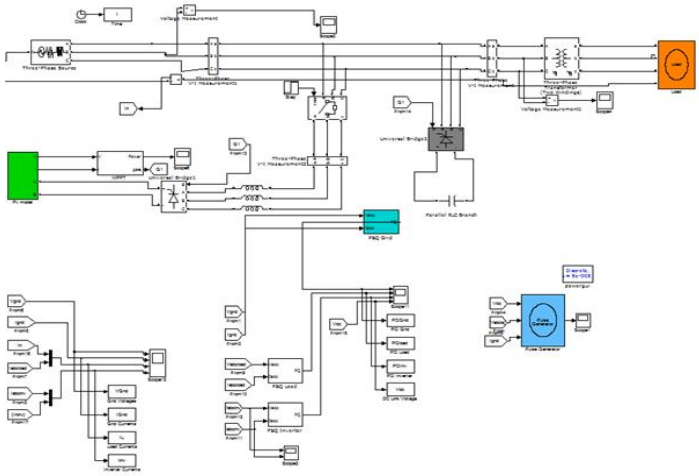

Fig4. PV generation and load protection using DVR system

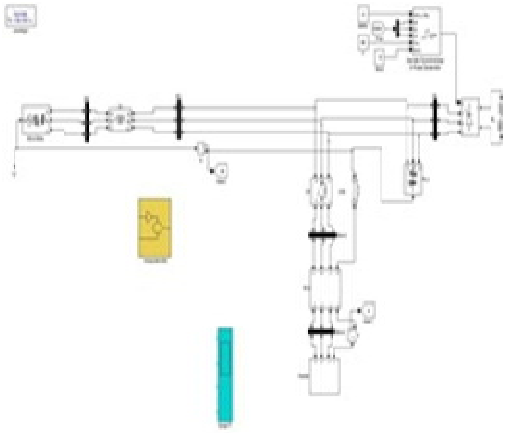

Fig5. Integration of PV and DVR system.

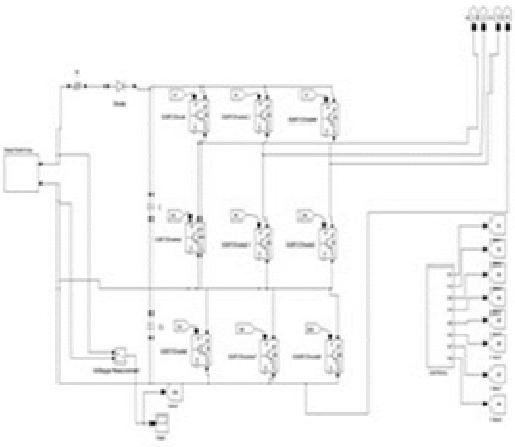

Fig6. 9-pulse with PV

The transmission losses due to various conditions are to be mitigated by the use of a DVR. Fig.4. The above model with six gate is upgraded to nine pulse bridge rectifier which is detailed hereafter as 9 pulse grid integrated PV – 9 pulse inverter model. Fig 5 Fig. 6 Table II and Table III

TABLE II
System Parameters

Parameter	Value
Grid voltage (L–L) (rms) V_{base}	735V
Line frequency	50 Hz
Nominal PV power (Base kVA)	10 kVA
Nominal load power	10 kVA
Nominal load power factor	0.8 lagging
DC link voltage	700 V
DC link capacitance	3000 µF
Maximum shunt current, (I_{sh-max})	20 A
Series transformer rating/turn ratio	10 kVA/ 1:1
Filter inductor L_f and capacitance C_f	5 mH and 50 µF
Grid impedance Z_{line}	$0.5 + j0.05\ \Omega$

TABLE III
Input and Output Values of Voltage

S.No	Type	Input	Output	THD
1	Without DVR	100v	50v	0.48%
2	With DVR	100v	100v	0.41%
3	9-pulse	500v, 400v	400v, 300v	0.09%

IV. RESULTS

Fig 7 Fig 8 Fig 9 Fig 10 Fig 11 Fig 12 Fig 13 Fig 14 Fig 15 Fig 16 Fig 17 From fig 7, fig 8 and fig 9 show the input , output wave forms with and without DVR, whereas the fig 10 shows the FFT analysis for the same. Fig 11 and Fig 12 gives us the voltage levels of the system with DVR, fig 13 and fig 14 are the results of simulation with DVR, fig 15 with FFT analysis with DVR and fig 16 shows the active and reactive power. From the results it is observed that voltage profile of the grid after implementing DVR is improved.

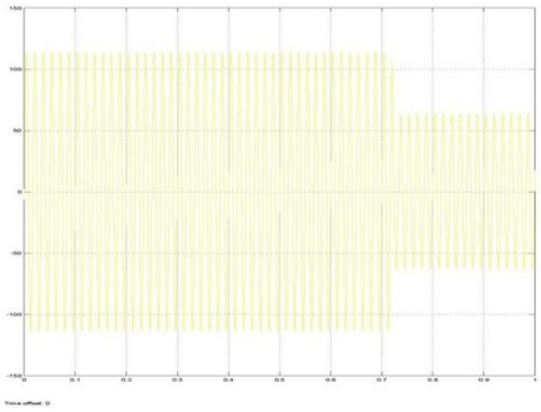

Fig7. Input voltage without DVR

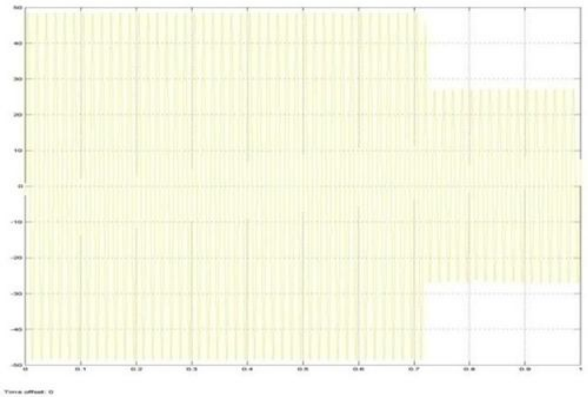

Fig8. Output voltage without DVR

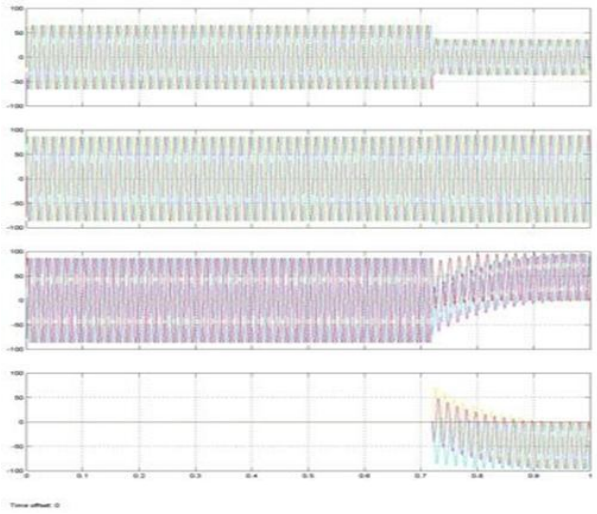

Fig9. Output waveforms without DVR

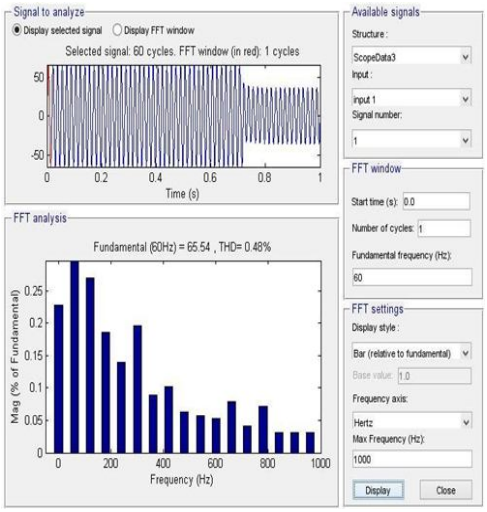

Fig10. THD Analysis for the system without DVR

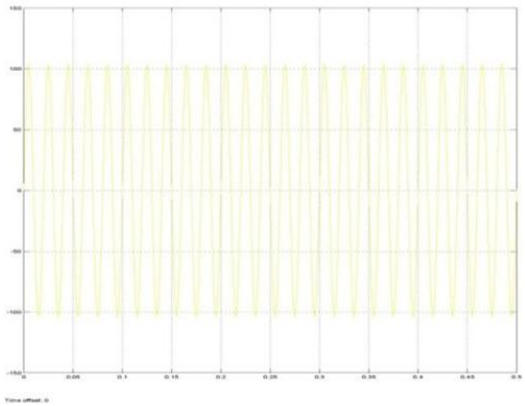

Fig11. Input Voltage with DVR

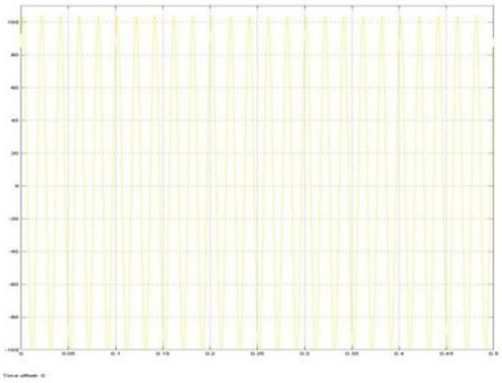

Fig 12. Output with DVR system

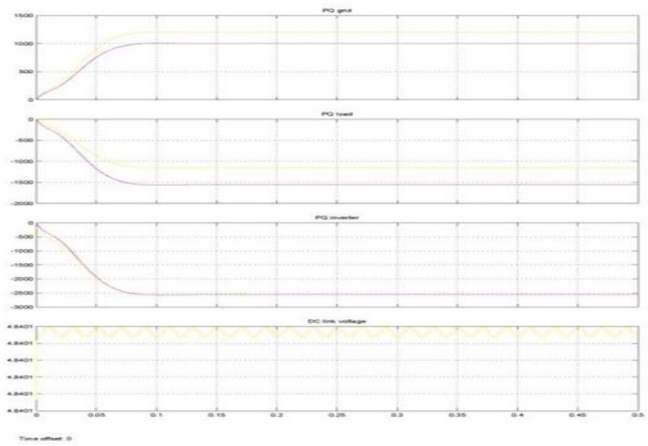

Fig13. Operation of system during health grid mode

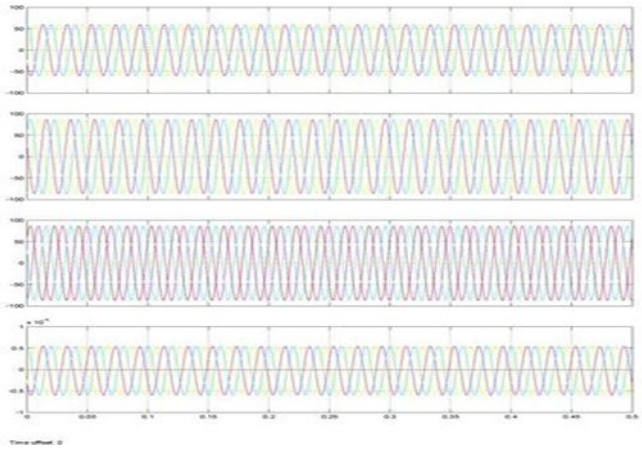

Fig14. Output waveforms with DVR system.

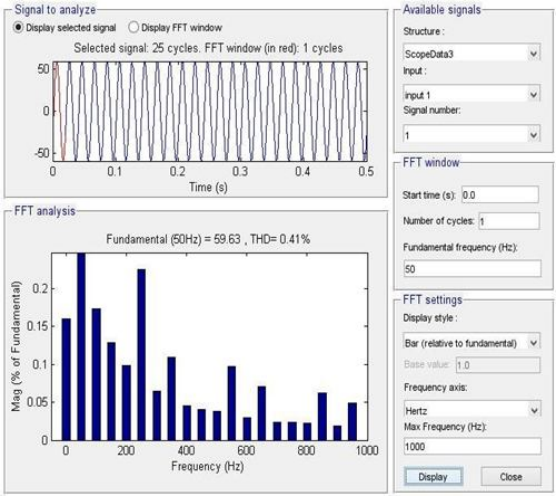

Fig15. THD Analysis for the system with DVR

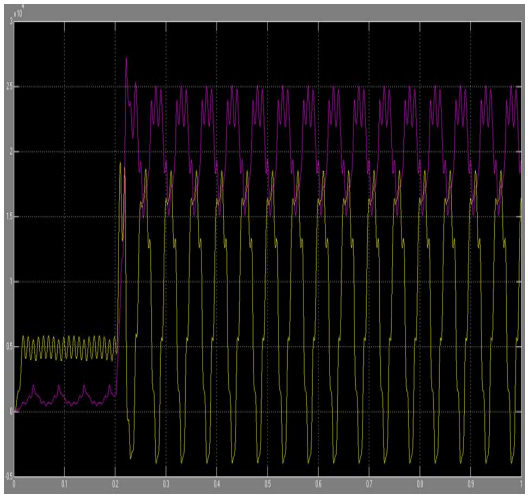

Fig 16. Active and Reactive power with DVR

V. CONCLUSION

In this paper, a conventional grid connected PV system with self-supported DVR is implemented with 9 pulse inverter mode. It is presented to enhance the functionalities of existing PV and DVR against grid faults. The proposed configuration can operate in different modes based on the grid condition and it reduces the basic operation of 12 pulse mode of operation into 9 pulse PV power generation mode to facilitate the enhanced THD analysis. The comprehensive simulation study and experimental validation demonstrate the effectiveness of the proposed configuration and its practical feasibility to perform under different operating conditions.

REFERENCES

[1] S. B. Kjaer, J. K. Pedersen, and F. Blaabjerg, "A review of single-phase grid-connected inverters for photovoltaic modules," IEEE Trans. Ind. Appl., vol. 41, no. 5, pp. 1292– 1306, Sep./Oct. 2005.
[2] T. Esram, J. W. Kimball, P. T. Krein, P. L. Chapman, and P. Midya, "Dynamic maximum power point tracking of photovoltaic arrays using ripple correlation control," IEEE Trans. Power Electron., vol. 21, no. 5, pp. 1282–1291, Sep. 2006.
[3] IEEE Recommended Practices and Requirements for Harmonic Control in Electrical Power Systems, IEEE Standard 519-1992, Apr. 1993, pp. 1–112.
[4] J. A. Martinez and J. M. Arnedo, "Voltage sag studies in distribution networks—Part I: System modelling," IEEE Trans. Power Del., vol. 21, no. 3, pp. 338–345, Jul. 2006.
[5] R. A. Walling, R. Saint, R. C. Dugan, J. Burke, and L. A. Kojovic, "Summary of distributed resources impact on power delivery systems," IEEE Trans. Power Del., vol. 23, no. 3, pp. 1636–1644, Jul. 2008.
[6] C. Meza, J. J. Negroni, D. Biel, and F. Guinjoan, "Energy-balance modeling and discrete control for single- phase grid-connected PV central inverters," IEEE Trans. Ind. Electron., vol. 55, no. 7, pp. 2734–2743, Jul. 2008.

[7] T. Shimizu, O. Hashimoto, and G. Kimura, “A novel high-performance utility-interactive photovoltaic inverter system,” IEEE Trans. Power Electron., vol. 18, no. 2, pp. 704–711, Mar. 2003. Electron., vol. 54, no. 4, pp. 2249–2261, Aug. 2007.
[8] Abdul mannan Rauf, and Vinod Khadikikar, ”Integrated Photovoltaic and Dynamic Voltage Restorer system Configuration” IEEE Trans. Sustainable Energy., vol. 6, no. 2, pp. 400–410, April. 2015.
[9] R. H. Salimin and M. S. A. Rahim, “Simulation Analysis of DVR Performance for Voltage Sag Mitigation” International Power Engineering and Optimization Conference (PEOCO2011), Shah Alam, Selangor, Malaysia, 6-7 June 2011.
[10] J. D. Li, S. S. Choi, and D. M. Vilathgamuwa, “Impact of voltage phase jump on loads and its mitigation,” in Proc. 4th Int. Power Electron, Motion Control Conf., Xian, China, Aug. 14–16, 2004, vol. 3, pp. 1762–1766.
[11] S. S. Choi, J. D. Li, and D. M. Vilathgamuwa, “A generalized vAoltage compensation strategy for mitigating the impacts of voltage sags/swells,” IEEE Trans. Power Del., vol. 20, no. 3, pp. 2289–2297, Jul. 2005.
[12] Y. W. Li, D. M. Vilathgamuwa, F. Blaabjerg, and P. C. Loh, “A robust control scheme for medium-voltage-level DVR implementation,” IEEE Trans. Ind.

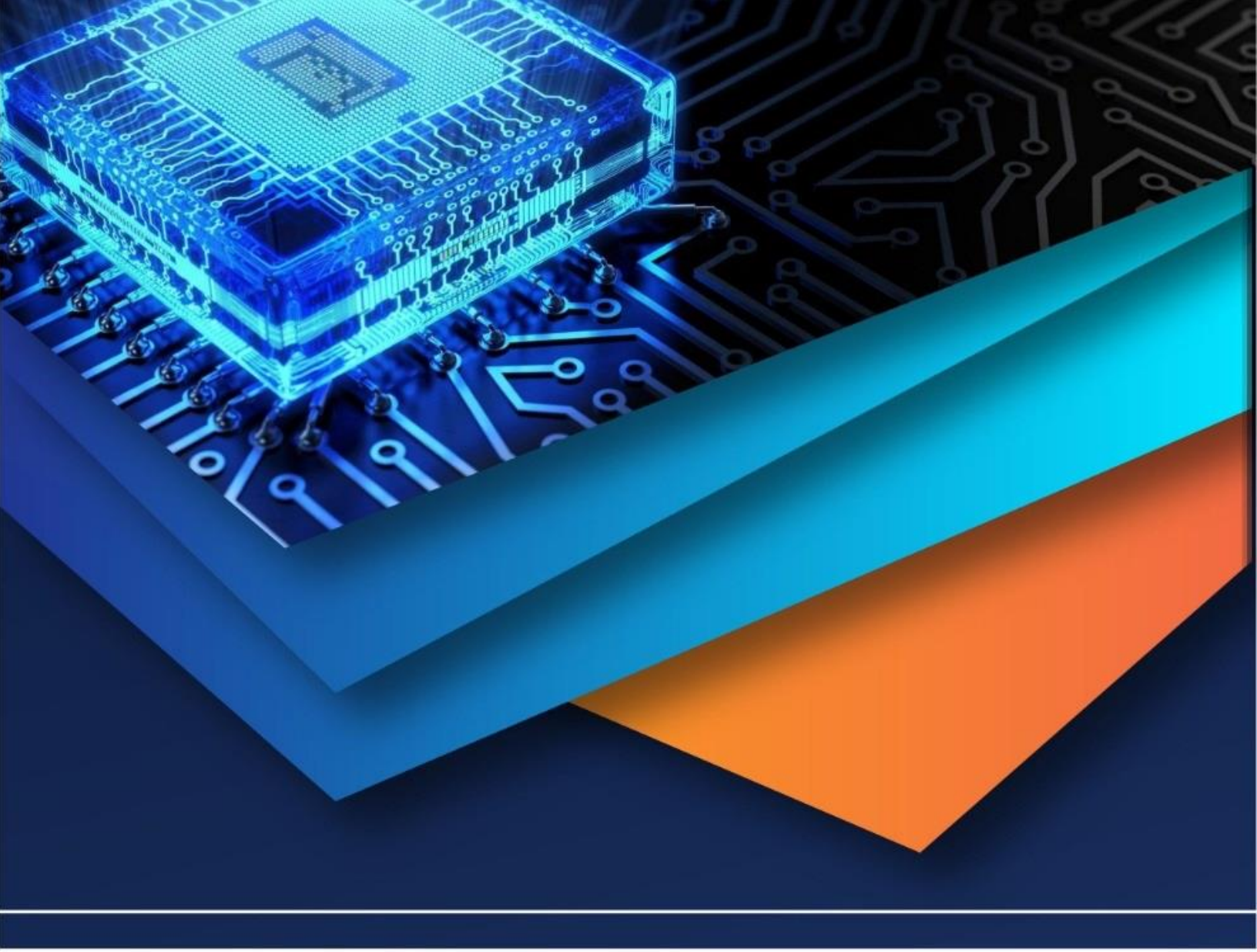

10.22214/IJRASET

45.98

IMPACT FACTOR: 7.129

IMPACT FACTOR: 7.429

INTERNATIONAL JOURNAL FOR RESEARCH

IN APPLIED SCIENCE & ENGINEERING TECHNOLOGY